ONLINE FIRST

This is a provisional PDF only. Copyedited and fully formatted version will be made available soon.

ISSN: 0015-5659

e-ISSN: 1644-3284

Possible protective and curative effects of selenium nanoparticles on testosterone-induced benign prostatic hyperplasia rat model

Authors: W. A. Elfakharany, M. M. Safwat, A. S. Essawy

DOI: 10.5603/FM.a2021.0113

Article type: Original article

Submitted: 2021-10-03

Accepted: 2021-10-21

Published online: 2021-10-28

This article has been peer reviewed and published immediately upon acceptance.
It is an open access article, which means that it can be downloaded, printed, and distributed freely, provided the work is properly cited.
Articles in "Folia Morphologica" are listed in PubMed.

Possible protective and curative effects of selenium nanoparticles on testosterone-induced benign prostatic hyperplasia rat model

W.A. Elfakharany et al., Selenium nanoparticles testosterone prostatic hyperplasia

W.A. Elfakharany[1], M.M. Safwat[1], A.S. Essawy[2, 3]

[1]Human Anatomy and Embryology Department, Faculty of Medicine, Ain Shams University, Cairo, Egypt

[2]Human Anatomy and Embryology Department, Faculty of Medicine, Menoufia University, Menoufia, Egypt

[3]Anatomy Department, Ibn Sina National College for medical Studies, Jeddah, Saudi Arabia

Address for correspondence: Asmaa Saeed Essawy, Faculty of Medicine, Menoufia University, Menoufia, Egypt & Ibn Sina National College for medical Studies, Almahjar street, Jeddah, Saudi Arabia, tel: 00966546637821, e-mail: doc_asmaa@hotmail.com

ABSTRACT

Background: Men over the age of 40 are more likely to develop benign prostatic hyperplasia (BPH). BPH is characterized by proliferation of the prostatic epithelium and stroma. Selenium nanoparticles (SeNPs), is an essential metalloid mineral and antioxidant. In this study, SeNPs were tested for their potential protective and curative impacts on BPH in rats.

Materials and methods: 50 male Sprague-Dawley rats were randomly divided into five groups: Group I (Control group); Group II (Orchiectomized group): bilateral orchiectomy was conducted on rats; Group III (BPH group): testosterone (TE) enanthate injection was used to induce BPH; Group IV (Protective group): rats were given SeNP before subjecting rats to BPH; Group V (Curative group): rats were succumbed to BPH, followed by administration of

SeNP. Measurement of prostate specific antigen (PSA) and TE in serum was performed and prostates were weighed and prepared for histological, immunohistochemical and ultrastructural examination.

Results: In the BPH group, serum TE- and PSA-levels, as well as prostate weight, increased significantly and significant decreases in the protective and curative groups. Reduced acinar lumen, expansion of stroma and epithelial hyperplasia were noticed in the BPH group, which were ameliorated significantly both in protective and curative groups. There was an increase in PCNA immunoreaction in the BPH group and a decrease in both the protective and curative groups. On TEM of BPH group, the nuclei appeared irregular with dilated endoplasmic reticulum, loss of cell boundaries and apical microvilli. The protective group showed more improvement than the curative group.

Conclusions: The effects of SeNPs on BPH induced by TE in rats, were both protective and curative, although the protective effects were more pronounced.

Key words: selenium nanoparticles, testosterone, benign prostatic hyperplasia, rat

INTRODUCTION

BPH is characterized by proliferation of the prostatic epithelium and the stroma, distinguished by an unregulated growth of the prostate [1]. The condition is common among men over 40 and 68% of males over the age of 50 have symptoms associated with the disease [2]. In more than 50% of males over the age of 60, classical BPH symptoms will manifest when stromal and epithelial cells proliferate in the transitional zone, which compresses the urethra [3, 4].

BPH is distinguished by an increase in volume of prostate caused by hyperplasia of stromal and epithelial cells impairing urine flow. Ultimately, this leads to polyuria, urinary retention, nocturia, urinary hesitancy, and increased risks for urinary tract infections [5]. While the pathogenesis of BPH remains an enigma, several lines of evidence have suggested that hormonal and vascular changes trigger prostatic cell proliferation and accelerate BPH development [6].

With age, the normal decline of androgen accompanied by a constant rise in estradiol results in an increase of the ratio of estradiol to testosterone (TE) [7]. This androgen-estrogen disparity, as well as the shift toward estrogen dominance, may be linked to growth of prostate. Furthermore, it is assumed that elevated androgen levels are essential for the development of BPH [8].

The 5 alpha reductase enzyme in the prostate converts TE to its active metabolite, dihydrotestosterone (DHT), which is a key mediator for growth of the prostate [9]. The pathophysiology of BPH has been linked to differentiation, apoptosis, and epithelial/stromal interaction. Transforming growth factor-β1 is an imperative pro-inflammatory cytokine that regulates cellular proliferation and apoptosis [10]. An increased expression of the angiogenic factor VEGF was also observed in patients with BPH [11].

The field of nanotechnology presents a host of potential applications in biology and biomedicine. Because of nanomaterials' unique properties, such as they are smaller, biocompatible, and able to penetrate cellular membranes to carry drugs, they are used in many biomedical applications [12].

Among the most important micronutrients for our health is selenium nanoparticles (SeNPs), an essential metalloid mineral and antioxidant. Selenium also has cancer chemo-preventive properties [13]. There is a strong association between selenium deficiency and many physiological disorders, such as higher cancer risks. Due to their low therapeutic index, different selenium supplements fail to restore selenium levels. In this regard, it would be advantageous to have a form of selenium that is less toxic with potential anti-cancer properties [14].

Considering the high health concerns associated with benign prostatic hyperplasia, our goal of this work was to illustrate, for the first time up to our knowledge, the possible ameliorative effects of selenium nanoparticles on benign prostatic hyperplasia induced by testesterone and to elucidate the underlying mechanisms through which selenium nanoparticles act based on biochemical, histological, immunohistochemical and ultrastructural studies.

MATERIALS AND METHODS

Chemicals

Induction of benign prostatic hyperplasia. TE enanthate injections intramuscularly (Cidoteston 250 mg ampoule, CID Company, Giza, Egypt) were used to induce BPH in rats once weekly, for five consecutive weeks, at a dose of 25 mg/rat [15]. To dilute the dose of TE, 100 µL of olive oil were used as the vehicle [16].

Selenium nano-particles (Nano Se, SeNPs). SeNPs were purchased from the Nano Tech Egypt for Photo-Electronics Communication Center, City of 6 October, Al-Giza, Egypt, in the form of orange suspension of concentration (7.8 ppm) and average size (20±25 nm) [17]. A daily dose of 0.1 mg/kg of SeNPs was administered orally by gavage for 14 days [18].

Animals

Through the entire study, 50 three-month-old male Sprague–Dawley rats weighing 200-250 g were utilized. Rats were bought from Animal House of Faculty of Medicine, Ain Shams University, Cairo, Egypt. They were acclimatized for two weeks in stainless steel cages prior to starting the experiment. They were kept in a climate-controlled room where they had 12 hours of light/dark cycles. The rats received access to tap water and rodent pellets as needed.

Experimental design

All experimental procedures and animal handling were carried out according to accepted animal care standards and approved by Ain Shams University's ethical committee. Following acclimatization, we divided the rats randomly into five groups (10 rats/group):

Group I (Control group): subdivided into group IA (negative control subgroup), where 100 µL of olive oil were administered each week for successive five weeks as a vehicle [15] and group IB (sham control subgroup), where incision, manipulation and stitching of the scrotum were done without resecting the testes [19].

Group II (Orchiectomized group): bilateral orchiectomy was performed on rats [20]. In order to prevent the influence of intrinsic TE, the operation took place seven days before BPH induction [15].

Group III (BPH group): in which TE enanthate was injected intramuscularly three days after orchiectomy once a week for five successive weeks to induce BPH [15].

Group IV (Protective group): in which rats were given SeNP (0.1 mg/ kg) daily by oral gavage for 14 days [18] before subjecting rats to benign prostatic hyperplasia through injection of TE enanthate intramuscularly for successive five weeks.

Group V (Curative group): in which BPH was induced by injection of TE enanthate intramuscularly for successive five weeks followed by SeNP treatment (0.1 mg/kg) by oral gavage for 14 days.

Rats were sacrificed at the end of the experiment and their prostates were instantly extracted, weighed and processed for histological, immunohistochemical and ultrastructural examination.

Orchiectomy procedures

Ketamine (90 mg/kg) and Xylazine (12 mg/kg) were intraperitoneally injected to induce anesthesia [21]. After confirming complete anesthesia, the testis and epididymal fat were gently removed through a ventral 1.5 cm incision on the scrotum, followed by ligation and cutting of the spermatic cord and testicular vessels. Incisions have been sutured using 4-0 silk sutures after both testes were removed [20]. An intraperitoneal dose of Ampicillin (4000 IU/kg) was given for three days as a prophylactic measure, and local application of Coloplast paste (Humlebaek, Denmark) was also administered.

Biochemical analysis

After the five weeks of the experiment, the rats were fasted overnight and then overdosed with Ketamine and Xylazine before they were sacrificed. To obtain the serum, we took blood samples directly from the abdominal aorta and centrifuged them for 15 minutes at

3000^{x}g. A testosterone ELISA kit (Biocheck, USA) and DHT ELISA kit (Abnova, USA) were used to measure TE and prostate specific antigen (PSA) in serum using an enzyme-linked immunosorbent assay (ELISA) [22, 23].

Prostate weight index

Prostate glands were carefully removed after scarification and weighed. Calculation of prostate weight (PW) index was done using this formula: PW index = (PW/Body weight) x 100 [24].

Evaluation of markers of prostate oxidative stress

To homogenize prostate tissues, ice-cold phosphate-buffered saline (50 mM potassium phosphate, pH 7.5) was used. The level of reduced glutathione (GSH) in tissues homogenates was measured using a kit available commercially (Biodiagnostic, Cairo, Egypt) [25]. Furthermore, a commercial kit (Biodiagnostic, Cairo, Egypt) was used to determine the catalase (CAT) and superoxide dismutase (SOD) activities. Lipid peroxidation has been measured spectrophotometrically by measuring malondialdehyde (MDA) level using thiobarbituric acid reactive substance (TBARS) method, following the description of Mihara and Uchiyama [26].

Histological study

Tissue samples from the prostate's ventral lobes were preserved for at least 24 hours in a 10% neutral buffered formalin solution prior to the fabrication of the paraffin blocks, the paraffin sections were then made at a thickness of 4 cm. A final step was to mount sections on glass slides and stained by Hematoxylin and Eosin (H & E) [27] and Masson's trichrome [28].

Immunohistochemistry

The paraffin sections on poly-L-lysin coated slides were deparaffinized and rehydrated. In order to inhibit endogenous peroxidase, the sections were immersed in 3%

hydrogen peroxide (H2O2). Microwave antigen retrieval procedure was used. The sections were incubated with primary anti-PCNA antibody, cellular regeneration marker, (Sigma-Aldrich, St Louis, Missouri, USA). Afterwards, the biotinylated polyvalent secondary antibody was applied. Next the sections were incubated in preformed streptavidin peroxidase. In the end, the DAB substrate chromogen (3,3′-diaminobenzidine tetrahydrochloride) was applied and the slides were counterstained with hematoxylin [29].

Morphometric study

A histomorphometric analysis was conducted for measurement of the epithelial height, the acinar luminal area, and the stromal area. To determine epithelial height, 30 lines per field were drawn through the acinar epithelium. To estimate the luminal area of an acinus, a line was drawn around its perimeter and then calculating the acinar area. In addition, the stromal area was calculated through subtraction of the acinar luminal area from the total area of the field. Luminal and stromal areas were measured using 100x magnification, whereas epithelium height was measured using 400x magnification [30].

Using a magnification of x400, the mean area percentage of PCNA was measured. To reduce inter-observer bias, a single blinded examiner conducted all histomorphometric analyses using Image J software. Each parameter was explored in ten non-overlapping fields for five different rats/experimental group.

Transmission electron microscopy

Small prostate specimens were immersed in 2.5 % buffered glutaraldehyde in 0.1 PBS at pH 7.4 and 4°C for 2 hours, then replaced with 1% osmium tetroxide in 0.1 mol/L for 1 hour. at 4°C to fix the specimens. Thereafter, specimens were dehydrated in ascending serial dilutions of ethanol (50, 70, 90, 95 and four times 100%, each for 30 minutes) followed by acetone dehydration for 30 minutes. Lastly, the fixed specimens were embedded in epoxy resin (Epoxy Embedding Medium Kit; Sigma). Using an ultramicrotome (RMC PT-XL PowerTome Ultramicrotome), semi- and ultra-thin sections were cut. Toluidine blue staining of semithin slices (1μm thick) was performed and the sections were examined using an Olympus BX61 light microscope. Ultrathin sections (70- 90 nm) were cut by ultramicrotome

then stained by 2% uranyl acetate as a principal stain and lead citrate as counter stain to be examined using JEM-1400 Plus (JEOL, Japan) transmission electron microscope at the Electron Microscope Unit, Faculty of Science, Alexandria University, Alexandria, Egypt [31].

Statistical analysis

In conducting the statistical analysis, we used the Statistical Package for the Social Sciences (SPSS) software (16.0; SPSS, Inc., Chicago, IL, USA). The data were expressed as mean±standard deviation (SD). One-way analysis of variance (ANOVA), followed by the Tukey's post-hoc test was used to analyze the data. P values ≤0.05 were considered to be significant.

RESULTS

Clinical observations

No mortality or behavioral changes were observed during the treatment period in any group. Also, no differences were observed in the general health status of the control and treated groups.

Biochemical analysis

The orchiectomized group showed a statistically significant decrease in TE and PSA serum levels, in comparison with control group. In comparison with control and orchiectomized groups, BPH group shows statistically significant increase. Protective and curative groups showed significant decreases in TE and PSA levels, compared to the BPH group. Furthermore, the protective group revealed a significant decrease in TE and PSA levels when compared with the curative group (Table 1).

Body and prostate weight changes

The difference in body weight gain between the groups was not statistically significant. BPH group showed statistically significant increases in PW and PW index, when

compared to the control group. In both protective and curative groups, SeNP administration significantly reduced the PW and PW index, compared with BPH group. Furthermore, a statistically significant decrease in the PW and the PW index was observed in orchiectomized group when compared with all other groups (Table 2).

Oxidative stress markers

In the BPH group, testosterone treatment increased MDA levels significantly compared to control group. SeNPs administration, either in a protective or curative group, significantly alleviated testosterone's effect on lipid peroxidation. Furthermore, the BPH group had significant decrease in GSH, SOD and CAT levels compared with control group. Nonetheless, both protective and curative groups that received nano-selenium had significant increases in GSH, SOD and CAT levels in comparison with the BPH group (Table 3).

Histopathological results

Sections of the control group stained with H&E, and Masson’s trichrome revealed normal prostate tissue, formed of numerous acini that appeared lined with a single layer of low columnar epithelium, and sparse stroma (Figure 1 A&F). In between the acini, fine collagen fibers were visible dispersed in the stroma (Figure 2A). The orchiectomized group exhibited an inflammatory infiltrate and expansion of stroma. In some acini, the epithelial cells were flattened or lost (Figure 1 B&G). Plentiful collagen fiber deposits could be seen in the stroma (Figure 2B). BPH group showed striking histological changes. Epithelial hyperplasia markedly narrowed the acinar lumens and produced large involutions. There was cell loss in some epithelial areas and other epithelial cells displayed vacuolations. Congested blood vessels were noticed in the stroma between acini as well (Figure 1 C&H). There was an abundance of collagen fibers in the stroma (Figure 2C). Both protective and curative groups displayed obvious improvement and restored many normal characteristics of the prostate. In the protective group, the acini appeared lined by low columnar epithelium with no involutions and reduced stromal thickness (Figure 1 D&I). There were also no involutions in the curative group, though some acini were lined by flat epithelium and others had multiple layers of epithelium accompanied by moderate amount of stroma (figure 1 E&J). Minimal amount of

collagen was found in the stroma of the protective group (Figure 2D), while curative group showed moderate levels of collagen fibers (Figure 2E). Accordingly, the protective group showed more improvement in histological characteristics than the curative group.

Immunohistochemical results

As a proliferation marker, immunohistochemical staining of PCNA in control tissue demonstrated minimal immunoexpression (Figures 3A). Moreover, PCNA expression in epithelial cells of the orchiectomized group was minimal (Figure 3B). In contrast, BPH group showed pronounced increase in nuclear PCNA immunoexpression in epithelial cells (Figure 3C). Both protective and curative group displayed minimal and moderate nuclear PCNA immunoexpression in the epithelial cells respectively (Figure 3D&E).

Morphometric results

A statistically significant reduction in epithelial height was seen in the orchiectomized group compared to the control group. In contrast, in the BPH group, there was a significant increase when compared to the control group along with the orchiectomized group. Conversely, when compared to the BPH group, treatment of SeNPs in the protective and curative groups led to a statistically significant decrease in epithelial height. Despite this, the epithelial height was clearly lower in the protective group, in comparison with the curative one, and was nearer the control values (Table 4).

A statistically significant reduction in luminal area was observed in both orchiectomized and BPH groups compared to the control group. Protective and curative groups showed significant increases in luminal area. This increase was not statistically significant in the curative group, but it was statistically significant in the protective group when compared to BPH one (Table 4).

The stromal area of the orchiectomized as well as the BPH groups was significantly increased when compared with the control group. The stromal area was statistically decreased when SeNPs were added to both the protective and curative groups. However, when compared to BPH, this decrease in stromal area was only significant in the protective group and non-significant in the curative group (Table 4).

In comparison with the control group, a significant increase in PCNA expression in the BPH group was found. On contrast, PCNA percentages decreased significantly in protective and curative groups, compared to BPH group. However, in protective group, PCNA percentage decreased significantly less than that in curative group (Table 4).

Transmission electron microscope results

In the control group, ultrathin sections of the ventral lobe of the prostate revealed normal epithelial cells with oval euchromatic nuclei and prominent nucleoli. A parallel flat endoplasmic reticulum (ER) and dense intracellular secretory vesicles can be seen in the cell cytoplasm. The acinar cells were separated by obvious cell membranes. As well as dense secretory vesicles, there were well-developed apical microvilli in the apical region of the cells (Figure 4).

Secretory cells of orchiectomized group are characterized by nuclei with irregular nuclear envelopes and hypodense chromatin. Rarified cytoplasm could be noticed. The boundaries of the cells were clearly defined. There was an absence of most secretory vesicles, but a few were hypodense and located at the apex of the cell. Most of the apical microvilli have been lost (Figure 5).

In the BPH group, multiple layers of secretory cells were seen. The nuclear envelopes of these cells were folded, with their ER was extremely dilated. Most of the cell boundaries were lost. Several variable sized intracellular vacuoles could be seen in the secretory cells. Secretory vesicles were rarely observed. The majority of the apical microvilli were missing (Figure 6).

Protective group revealed secretory cells arranged in one layer with normal nuclei, but their nuclear envelopes had slight invagination. The cytoplasm contained secretory vesicles and had slightly dilated ER. Moreover, the cells had distinct cell boundaries. Microvilli were largely restored to normal and secretory vesicles were also increased apically (Figure 7).

In the curative group, secretory cells' nuclei appeared irregular, having condensed chromatin and invaginations on their nuclear envelopes. Though, ER cisterns were somewhat dilated. Additionally, the cells' boundaries were still indistinct. There were some losses in the apical microvilli and some short microvilli. Apical secretory vesicles were also evident in some cells (Figure 8).

DISCUSSION

BPH is the most common benign tumor in men, which increases with aging [32]. BPH presents with symptoms of urinary retention and voiding difficulties, which negatively affect patients' quality of life. Furthermore, there are several dangerous complications associated with BPH, including urinary tract infections, gross hematuria, acute urinary retention, along with renal failure [33].

BPH's etiology is very arguing [34]. The pathogenesis of BPH is still unclear, but numerous factors, such as hormones, inflammation, growth factors, and metabolism disorders, appear to contribute to its progress [35].

According to our best knowledge, this is the first work to demonstrate protective and curative effects of selenium nanoparticles on BPH induced by testosterone in rats using biochemical, histological, immunohistochemical, morphometric and transmission electron microscopic analysis.

In the current work, prostate glands of orchiectomized group revealed atrophy of the epithelium associated with increase in the stromal mass. Furthermore, following five weeks of TE injections, orchiectomized rats developed histopathological signs of BPH, taking the form of massive epithelial hyperplasia, acinar lumens reduction and stromal expansion, as well as marked deposition of collagen, that were more ameliorated in the protective group than in the curative one. In agreement with these findings, Nasr El-Din and Abdel Fattah [36] reported that castration in rats resulted in decrease in thickness of the epithelium. In addition, Jang et al. [15] reported that five weeks of intramuscular TE injection resulted in hyperplasia of epithelial cells and excessive development of prostate tissue.

Moreover, Minutoli et al. [37] showed that TE propionate injection completely deranged the prostate tissue and caused severe hyperplasia compared with control animals. The majority of these pathological features improved with selenium treatment coinciding with TE injection. They added that selenium (Se) and lycopene combining with serenoa repens reduces prostate hyperplasia most effectively. In addition, Lindshield et al. [38] reported that selenium decreased prostate adenocarcinoma growth in male rats. Also, lentinan-functionalized selenium nanoparticles combined with Zoledronic Acid have a good antitumor

effect on prostate cancer, according to An and Zhao [39]. Furthermore, Barbanente et al. [40] showed that platinum-loaded, selenium-doped hydroxyapatite nanoparticles selectively reduce proliferation of prostate and breast cancer cells without reducing proliferation of bone marrow stem cells.

Nanominerals are minerals that have been made into nanoparticles through the use of nanotechnology. A few studies have been done to check the effectiveness of nanominerals [41]. It is demonstrated that nanoparticles have unique properties including large surface areas, high surface activity, many surface-active centers, high catalytic efficiency, low toxicity, and high absorbed ability [42]. Due to their high biological efficacy, elemental Se nanoparticles (NSe) have recently drawn considerable interest. When compared to routine Se, its efficacy is primarily attributed to its high bioavailability, high surface activity, and low toxicity [43]. NSe has been used as a nutritional supplement and for medical therapy because of its high stability and nano-defined size in the redox state of zero [44]. In comparison to inorganic or organic Se, NSe would be more effective as a dietary supplement [41].

In the current study, the MDA levels were higher in rats treated with TE while the levels of SOD, catalase and GSH were lower in comparison with the control group. These results are in harmony with Kim et al. [45] who found significant increase of MDA and significant decrease of SOD, catalase and GSH levels in the prostate of rats administered testosterone. The authors attributed these findings to oxidative damage within the tissue of prostate induced by testosterone administration. In the present study, Nano-selenium treatment of rats before and after testosterone exposure appeared to restore prostate antioxidant activity by reverting the GSH, MDA concentration, catalase and SOD activities to nearly normal levels. The same findings were reported by Dkhil et al. [46] who found that SeNPs restored antioxidant enzyme activity and reduced lipid peroxidation and nitric oxide levels in the testis of streptozotocin-induced diabetic rats.

PCNA is a cell proliferation marker, as well as a cofactor of DNA polymerase delta, which is involved in replicating, excising, and repairing DNA [47]. Oxidative stress is believed to be mediated by the mechanisms that are involved in prostate proliferation [48]. By regulating transcription of target genes, eukaryotic nuclear factor kappa B (NF-κB) encourages cell proliferation [49]. In accordance with our results, Nasr El-Din and Abdel Fattah [36] showed that PCNA-positive cells were significantly increased in prostate tissue

following TE. Additionally, in the current work, selenium nanoparticles decreased the percentage of PCNA-positive cells. However, selenium nanoparticles were more effective in decreasing PCNA expression in the protective group than in the curative group. Our results were harmonic with Dkhil et al. [46] who found that streptotocin-induced diabetic rats treated with SeNPs showed abundant PCNA-positive cells in their testes, indicating strong PCNA expression.

Regarding the morphometric measurements in the present study, revealed decreased acinar luminal area, but increased prostate epithelial height and stromal area in BPH group. Similarly, Bharali & Chetry [50] demonstrated that 21 days of subcutaneous TE injections significantly increased epithelial height compared to control group. Likewise, Gonzales et al. [30] reported that TE administration increased the stromal area in mice, which is in agreement with our results. On the contrary, Gonzales et al. [30] showed that epithelium height did not change significantly after treatment with TE and significantly increased the acinar area compared to control group which was opposing to our findings.

In the present work, ultrathin examination of prostate specimens exhibited dilatation of ER, irregular nuclei, loss of cell boundaries, loss of apical microvilli, and mostly absent secretory vesicles after five weeks of TE injection after bilateral orchiectomy. Similar findings have been reported by Nasr El-Din and Abdel Fattah [36] who examined epithelial prostatic hyperplasia ultrastructure induced by testosterone. They reported that the nuclear envelopes of the secretory cells were infolded and the ER was dilated. Multiple intracellular vacuolations of various sizes appeared in the secretory cell. The majority of apical microvilli were lost.

An important contributor to BPH is prostate inflammation [51]. High-grade prostatic inflammation is significantly associated with larger prostate volumes and worse symptom scores in BPH patients [52]. In many experimental studies, testosterone induced BPH was shown to be mediated by inflammation, and protective agents have been found to reduce inflammation [53]. In prostatic tissue, DHT accumulation is adequate to cause imbalance between proliferation and apoptosis, as it increases expression of androgen-dependent growth factors, along with, by genomic and nongenomic stimulation of the NF κB /p65 signaling pathways, producing inflammatory cytokines expression [54,55]. The family of NF-κB transcription factors controls gene expression in inflammatory and immune responses, also, in the development and growth of cells [55,56].

A number of signaling intermediates participate in the transduction of downstream signals by IL-17 as it binds to its receptor. Activation of Act1 and TNF receptor-associated factor 6 (TRAF6) E3 ubiquitin ligases is an early event. As a result, they can stimulate degradation of the IκB inhibitor and also promote nuclear translocation of the transcription factor NF-κB [57]. Studies have shown that IL-17 is not expressed in healthy prostates but is found in BPH [54]. Androgens have been shown to reduce inflammation of the prostate. Anti-androgens result in inflammatory reactions of the prostate; mouse experiments have demonstrated this as well [58]. Possibly, this may explain why inflammatory responses in prostate tissue in the orchiectomized group were caused by decreased TE serum levels.

In fact, both IL-6 and IL-8 have been shown to promote proliferation of stromal BPH cells through trans differentiation of fibroblasts to myofibroblasts as well as motivation of basic fibroblast growth factor secretion indirectly that can stimulate prostatic growth effectively [59]. Furthermore, TNF-α plays a serious role in inflammation, cellular differentiation, proliferation and death [60].

SeNPs have been shown to inhibit MAP kinase, NF-κB and decrease TNF-α levels [61]. According to another study, SeNPs showed anti-inflammatory effects in multiple animal models [62]. According to Vunta et al. [63], Se increases an endogenous inhibitor of IKK, which resulted in inhibition of NF-κB. Se may also inhibit NF-κB activation through increasing the expression of GPx genes and inhibiting NF- κB phosphorylation through the redox pathway [63]. This could explain SeNPs' beneficial effects on BPH induced by TE in the existing work. Treatment with SeNPs to the protective group gave better results than to the curative group, likely due to the fact that early treatment inhibited NF-κB pathway activation.

Limitations and clinical implications

Other studies of longer duration and multiple dosages of selenium nanoparticles are needed to uncover its potential therapeutic benefits for benign prostatic hyperplasia. Clinical trials on humans should also be undertaken.

CONCLUSIONS

It was shown in the present study that SeNPs had both curative and protective actions on BPH in rats induced by TE, though it was more apparent that the protective effect outweighed the curative effect.

REFERENCES

1. Winner K, Polycarp O, Ifeoma I, et al. Effect of fractions of Kolaviron on some indices of benign prostatic hyperplasia in rats: identification of the constituents of the bioactive fraction using GC-MS. RSC Adv. 2016; 6(97): 94352–94360, doi: 10.1039/C6RA18266F.
2. de Sousa VP, Crean J, Borges VRA, et al. Nanostructured systems containing babassu (Orbignya speciosa) oil as a potential alternative therapy for benign prostatic hyperplasia. Int J Nanomedicine. 2013; 8: 3129–3139, doi: 10.2147/IJN.S47731.
3. Choi HM, Jung Y, Park J, et al. Cinnamomi cortex (Cinnamomum verum) suppresses testosterone-induced benign prostatic hyperplasia by regulating 5α-reductase. Sci Rep. 2016; 6: 31906, doi: 10.1038/srep31906.
4. Chughtai B, Forde JC, Thomas DD, et al. Benign prostatic hyperplasia. Nat Rev Dis Primers. 2016; 2:16032, doi: 10.1038/nrdp.2016.31.
5. Dinarvand R, Sepehri N, Manoochehri S, et al. Polylactide-co-glycolide nanoparticles for controlled delivery of anticancer agents. Int J Nanomedicine. 2011; 6:877–895, doi: 10.2147/IJN.S18905.
6. Briganti A, Capitanio U, Suardi N, et al. Benign prostatic hyperplasia and its aetiologies. Eur Urol Suppl. 2009; 8(13):865–871, doi:10.1016/j.eursup.2009.11.002.
7. La Vignera S, Condorelli RA, Russo GI, et al. Endocrine control of benign prostatic hyperplasia. Andrology. 2016; 4(3): 404–411, doi: 10.1111/andr.12186.
8. Sayeed QA, Khatoon F, Bahmed F, et al. Effect of testosterone and estrogen ratio: an indicator of benign prostatic hyperplasia (BPH). Indian J Clin Anat Physiol. 2016; 3(2): 125–130, doi: 10.5958/2394-2126.2016.00030.X.
9. Park E, Lee MY, Jeon WY, et al. Inhibitory effect of Yongdamsagan-tang water extract, a traditional herbal formula, on testosterone-induced benign prostatic hyperplasia in rats. Evid Based Complement Alternat Med. 2016; 2016:1428923, doi: 10.1155/2016/1428923.
10. Descazeaud A, Weinbreck N, Robert G, et al. Transforming growth factor β-receptor II protein expression in benign prostatic hyperplasia is associated with prostate volume and inflammation. BJU Int. 2011;108(2b): E23–E28, doi:10.1111/j.1464-410X.2010.09699.x.
11. Sciarra A, Voria G, Mariotti G, et al. Histopathological aspects associated with the diagnosis of benign prostatic hyperplasia: clinical implications. Urol Int. 2002;69 (4): 253–262, doi:10.1159/000066128.
12. Wang EC, Wang AZ. Nanoparticles and their applications in cell and molecular biology. Integr Biol. 2014;6(1): 9–26, doi:10.1039/c3ib40165k.
13. Arvizo RR, Rana S, Miranda OR, et al. Mechanism of anti-angiogenic property of gold nanoparticles: role of nanoparticle size and surface charge. Nanomedicine. 2011;7(5): 580–587, doi:10.1016/j.nano.2011.01.011.

14. Sonkusre P. Specificity of Biogenic Selenium Nanoparticles for Prostate Cancer Therapy with Reduced Risk of Toxicity: An in vitro and in vivo Study. Front Oncol. 2020;9: 1541, doi: 10.3389/fonc.2019.01541.

15. Jang H, Bae WJ, Yuk SM, et al. Seoritae extract reduces prostate weight and suppresses prostate cell proliferation in a rat model of benign prostate hyperplasia. Evid Based Complement Alternat Med. 2014; 2014: 475876, doi: 10.1155/2014/475876.

16. Bian Q, Wang W, Wang N, et al. Quantification of arachidonic acid and its metabolites in rat tissues by UHPLC-MS/MS: application for the identification of potential biomarkers of benign prostatic hyperplasia. PLoS One. 2016;11(11): e0166777, doi: 10.1371/journal.pone.0166777.

17. Lide DV. Handbook of Chemistry and Physics. 2002, 83rd ed., CRC Press, Clevland, (Chapter 2).

18. Al-Quraishy S, Dkhil MA, Abdel Moneim AE. Anti-hyperglycemic activity of selenium nanoparticles in streptozotocin-induced diabetic rats. Int J Nanomedicine. 2015;10: 6741-56, doi: 10.2147/IJN.S91377.

19. Zhong X, Lin J, Zhou J, et al. Anti-proliferative effects of Qianliening capsules on prostatic hyperplasia *in vitro* and *in vivo*. Mol Med Rep. 2015; 12(2): 1699–1708, doi: 10.3892/mmr.2015.3566.

20. Lee MY, Shin IS, Lee NH, et al. Effects of Platycodon grandiflorum methanolic extract on testosterone-induced benign prostatic hyperplasia in Wistar rats. Afr J Biotechnol. 2012; 11(77): 14186–14192, doi: 10.5897/ajb12.804.

21. Soliman HM, Abd El-Haleem MR, El Tarhouny SA. Histomorphometrical and electron microscopic study of adrenocorticocytes following surgically induced extrahepatic biliary obstruction in adult female albino rats. Folia Biol (Praha). 2015; 61(1): 14–25, PMID: 25958307.

22. Peng CC, Liu JH, Chang CH, et al. Action mechanism of Ginkgo biloba leaf extract intervened by exercise therapy in treatment of benign prostate hyperplasia. Evid Based Complement Alternat Med. 2013;2013: 408734, doi: 10.1155/2013/408734.

23. Lee G, Shin J, Choi H, et al. Cynanchum wilfordii ameliorates testosterone-induced benign prostatic hyperplasia by regulating 5α-reductase and androgen receptor activities in a rat model. Nutrients. 2017; 9(10): 1070, doi: 10.3390/nu9101070.

24. Vyas BA, Desai NY, Patel PK, et al. Effect of Boerhaavia diffusa in experimental prostatic hyperplasia in rats. Indian J Pharmacol. 2013, 45(3): 264–269, doi: 10.4103/0253-7613.111946.

25. Tietze F. Enzymic method for quantitative determination of nanogram amounts of total and oxidized glutathione: applications to mammalian blood and other tissues. Anal Chem. 1969;27: 502–522, doi: 10.1016/0003-2697(69)90064-5.

26. Mihara M, Uchiyama M. Determination of malonaldehyde precursor in tissues by thiobarbituric acid test. Anal Biochem. 1978;86: 271–278, doi: 10.1016/0003-2697(78)90342-1.

27. Bancroft JD, Layton C. The hematoxylins and eosin. In: Suvarna SK, Layton C, Bancroft JD (eds). Bancroft's theory and practice of histological techniques. 8th edition, Churchill Livingstone, Elsevier, China, 2018, 126–138.

28. Bancroft JD, Layton C. Connective and other mesenchymal tissues with their stains. In: Suvarna SK, Layton C, Bancroft JD (eds). Bancroft's theory and practice of histological techniques. 8th edition, Churchill Livingstone, Elsevier, China, 2018, 153–175.

29. Bancroft JD, Layton C. immunohistochemical and immunofluorescent techniques. In: Suvarna SK, Layton C, Bancroft JD (eds). Bancroft's theory and practice of histological techniques. 8th edition, Churchill Livingstone, Elsevier, China. 2018, 337–394.

30. Gonzales GF, Gasco M, Malheiros-Pereira A, et al. Antagonistic effect of Lepidium meyenii (red maca) on prostatic hyperplasia in adult mice. Andrologia. 2008;40(3): 179–185, doi: 10.1111/j.1439-0272.2008.00834.x.

31. Woods AE, Stirling JW. Transmission electron microscopy. In: Suvarna SK, Layton C, Bancroft JD (eds). Bancroft's theory and practice of histological techniques. 8th edition, Churchill Livingstone, Elsevier, China, 2018, 434–475.

32. Donnell RF. Benign prostate hyperplasia: a review of the year's progress from bench to clinic. Curr Opin Urol. 2011;21(1): 22-6, doi: 10.1097/mou.0b013e32834100dd.

33. Li J, Tian Y, Guo S, et al. Testosterone-induced benign prostatic hyperplasia rat and dog as facile models to assess drugs targeting lower urinary tract symptoms. PLoS One. 2018;13(1): e0191469, doi: 10.1371/journal.pone.0191469.

34. Yang Y, Hu S, Liu J, et al. CD8+ T cells promote proliferation of benign prostatic hyperplasia epithelial cells under low androgen level via modulation of CCL5/STAT5/CCND1 signaling pathway. Sci Rep. 2017; 7: 42893, doi: 10.1038/srep42893.

35. Wang CT, Wang YY, Liu WS, et al. Rhodobacter sphaeroides extract Lycogen™ attenuates testosterone induced benign prostate hyperplasia in rats. Int J Mol Sci. 2018; 19(4): 1137, doi: 10.3390/ijms19041137.

36. Nasr El-Din WA, Abdel Fattah IO. The potential curative and preventive effects of garlic on testosterone-induced benign prostatic hyperplasia in orchiectomized rats. Rom J Morphol Embryol. 2019; 60(1): 145–158, PMID: 31263839.

37. Minutoli L, Altavilla D, Marini H, et al. Inhibitors of apoptosis proteins in experimental benign prostatic hyperplasia: effects of serenoa repens, selenium and lycopene. J Biomed Sci. 2014; 21(1): 19, doi:10.1186/1423-0127-21-19.

38. Lindshield BL, Ford NA, Canene-Adams K, et al. Selenium, but Not Lycopene or Vitamin E, Decreases Growth of Transplantable Dunning R3327-H Rat Prostate Tumors. PLoS one. 2010; 5(4): e10423, doi: 10.1371/journal.pone.0010423.

39. An Y, Zhao J. Functionalized Selenium Nanotherapeutics Synergizes With Zoledronic Acid to Suppress Prostate Cancer Cell Growth Through Induction of Mitochondria-Mediated Apoptosis and Cell Cycle S Phase Arrest. Front Oncol. 2021; 11:685784, doi: 10.3389/fonc.2021.685784.

40. Barbanente A, Nadar RA, Esposti LD, et al. Platinum-loaded, selenium-doped hydroxyapatite nanoparticles selectively reduce proliferation of prostate and breast cancer cells co-cultured in the presence of stem cells. J Mater Chem B. 2020; 8(14):2792-2804, doi: 10.1039/d0tb00390e.

41. Abdelnour SA, Alagawany M, Hashem NM, et al. Nanominerals: Fabrication Methods, Benefits and Hazards, and Their Applications in Ruminants with Special Reference to Selenium and Zinc Nanoparticles. Animals (Basel). 2021;11(7): 1916, doi: 10.3390/ani11071916.

42. Zhang JS, Wang XF, Xu TW. Elemental selenium at nano size as a potential chemoprotective agent with reduced risk of selenium toxicity: comparison with Se-methylselenocysteine in mice. Toxicol Sci. 2008; 101(1): 22–31, doi: 10.1093/toxsci/kfm221.

43. El-Deep MH, Ijiri D, Ebeid TA, et al. Effects of dietary nano-selenium supplementation on growth performance, antioxidative status, and immunity in broiler chickens under thermoneutral and high ambient temperature conditions. J Poult Sci. 2016; 53: .274–283, doi: 10.2141/jpsa.0150133.

44. El-Ramady HR, Domokos-Szabolcsy E, Abdalla NA, et al. Selenium and nano-selenium in agroecosystems. Environ Chem Lett. 2014; 12(4): 495–510, doi: 10.1007/s10311-014-0476-0.

45. Kim K, Yang H, Chang S, et al. Potential repositioning of GV1001 as a therapeutic agent for testosterone-induced benign prostatic hyperplasia. Int J Mol Med. 2018;42(4): 2260-2268, doi: 10.3892/ijmm.2018.3759.

46. Dkhil M, Zrieq R, Al-Quraishy S, et al. Selenium Nanoparticles Attenuate Oxidative Stress and Testicular Damage in Streptozotocin-Induced Diabetic Rats. Molecules. 2016; 21(11): 1517, doi:10.3390/molecules21111517.

47. Kanter M, Aktas C, Erboga M. Curcumin attenuates testicular damage, apoptotic germ cell death, and oxidative stress in streptozotocin-induced diabetic rats. Mol. Nutr. Food Res. 2013;57: 1578–1585, doi: 10.1002/mnfr.201200170.

48. Aydin A, Arsova-Sarafinovska Z, Sayal A, et al. Oxidative stress and antioxidant status in non-metastatic prostate cancer and benign prostatic hyperplasia. Clin Biochem. 2006; 39(2) : 176 -179, doi: 10.1016/j.clinbiochem.2005.11.018.

49. Shukla S, Shankar E, Fu P, et al. Suppression of NF-κB and NF-κB-regulated gene expression by apigenin through IκBα and IKK pathway in TRAMP mice. PLoS One. 2015; 10(9): e0138710, doi: 10.1371/journal.pone.0138710.

50. Bharali MK, Chetry LB. Aqueous methanolic bark extract of Oroxylum indicum inhibited testosterone induced prostate hyperplasia in rat. Phcog J. 2014; 6(3): 79–85, doi:10.5530/pj.2014.3.12.

51. Gandaglia G, Briganti A, Gontero P, et al. The role of chronic prostatic inflammation in the pathogenesis and progression of benign prostatic hyperplasia (BPH). BJU Int. 2013;112(4): 432-41, doi: 10.1111/bju.12118.

52. Robert G, Descazeaud A, Nicolaïew N, et al. Inflammation in benign prostatic hyperplasia: a 282 patients' immunohistochemical analysis. Prostate. 2009; 1;69(16): 1774-1780, doi: 10.1002/pros.21027.

53. Sayed RH, Saad MA, El-Sahar AE. Dapoxetine attenuates testosterone-induced prostatic hyperplasia in rats by the regulation of inflammatory and apoptotic proteins. Toxicol Appl Pharmacol. 2016; 311: 52–60, doi: 10.1016/j.taap.2016.09.024.

54. Krušlin B, Tomas D, Džombeta T, et al. Inflammation in prostatic hyperplasia and carcinoma – basic scientific approach. Front Oncol. 2017; 7: 77, doi: 10.3389/fonc.2017.00077.

55. Liu MC, Chen WH, Chiou CS, et al. Inhibition of chronic prostate inflammation by hyaluronic acid through an immortalized human prostate stromal cell line model. PLoS One. 2017; 12(5): e0178152, doi: 10.1371/journal.pone.0178152.

56. Austin DC, Strand DW, Love HL, et al. NF-κB and androgen receptor variant expression correlate with human BPH progression. Prostate. 2016; 76(5): 491–511, doi: 10.1002/pros.23140.

57. Cruz JA, Childs EE, Amatya N, et al. IL-17 signaling triggers degradation of the constitutive NF-κB inhibitor ABIN-1. ImmunoHorizons. 2017; 1(7): 133–141, doi: 10.4049/immunohorizons.1700035.

58. Bushman WA, Jerde TJ. The role of prostate inflammation and fibrosis in lower urinary tract symptoms. Am J Physiol Renal Physiol. 2016;311(4): F817–F821, doi: 10.1152/ajprenal.00602.2015.

59. Durak I, Yilmaz E, Devrim E, et al. Consumption of aqueous garlic extract leads to significant improvement in patients with benign prostate hyperplasia and prostate cancer. Nutr Res. 2003; 23(2): 199–204, doi:10.1016/S0271-5317(02)00495-5.

60. Malinen M, Niskanen EA, Kaikkonen MU, et al. Crosstalk between androgen and pro-inflammatory signaling remodels androgen receptor and NF-κB cistrome to reprogram the prostate cancer cell transcriptome. Nucleic Acids Res. 2017; 45(2): 619–630, doi: 10.1093/nar/gkw855.

61. Miroliaee AE, Esmaily H, Vaziri-Bami A, et al. Amelioration of experimental colitis by a novel nanoselenium–silymarin mixture. Toxicol Mech Methods. 2011;21(3): 200-8, doi: 10.3109/15376516.2010.547887.

62. El-Ghazaly MA, Fadel N, Rashed E, et al. Anti-inflammatory effect of selenium nanoparticles on the inflammation induced in irradiated rats. Can J Physiol Pharmacol. 2017;95(2): 101-110, doi: 10.1139/cjpp-2016-0183.

63. Vunta H, Davis F, Palempalli UD, et al. The anti-inflammatory effects of selenium are mediated through 15-deoxy-delta12,14-prostaglandin J2 in macrophages. J Biol Chem. 2007;282(25): 17964-17973, doi: 10.1074/jbc.M703075200.

Group	TE serum levels (ng/ml)	PSA (ng/ml)
Control group	4.04±0.5 [c]	4.65±0.24 [c]
Orchiectomized group	0.05±0.02 [d]	3.29±0.15 [d]
BPH group	12.67±0.7 [a]	10.25±0.40 [a]
Protective group	4.74±1.44 [c]	4.97±0.25 [c]
Curative group	8.15±1.06 [b]	5.65±0.54 [b]

Table 1. TE and PSA levels changes

a, b, c & d: There is significant difference (P>0.05) between any two groups, within the same column not having the same superscript letter.

Values are mean±SD. TE: Testosterone; PSA: Prostate specific antigen; BPH: Benign prostatic hyperplasia. Statistical analysis was performed by ANOVA, followed by Tukey's post-hoc test. SD: Standard deviation; ANOVA: Analysis of variance.

Table 2. Body weight, PW and PW index changes

Group	Initial body weight (g)	Final body weight (g)	Body weight gain (g)	PW (mg)	PW index
Control group	207.22±2.8	290.53±4.71	82.7±5.48 [a]	510±30.5 [d]	0.175±0.011 [d]
Orchiectomized group	218.22±3.85	306.35±7.65	88.10±7.43 [a]	100±19.6 [e]	0.326±0.006 [e]
BPH group	230.89±15.3	312.00±4.12	82.0±18.14 [a]	1365±215.4 [a]	0.439±0.067 [a]
Protective group	225.54±10.55	315.47±2.83	90±12.02 [a]	690±64.9 [c]	0.219±0.021 [c]
Curative group	235.22±6.91	321.5±13.34	86.30±7.54 [a]	840±28.9 [b]	0.261±0.077 [b]

a, b, c, d & e: There is significant difference (P>0.05) between any two groups, within the same column not having the same superscript letter.

Values are mean±SD. PW: Prostate weight; BPH: Benign prostatic hyperplasia. Statistical analysis was performed by ANOVA, followed by Tukey's post-hoc test. SD: Standard deviation; ANOVA: Analysis of variance.

Table 3. Markers of oxidative stress in the prostate

Group	MDA (nmol/mg protein)	GSH (mmol/mg protein)	SOD (U/mg protein)	CAT (U/mg protein)
Control group	0.235±0.063 [d]	0.135±0.010 [b]	40.5±2.45 [a]	0.56±0.045[a]
Orchiectomized group	0.252±0.075 [d]	0.152±0.008[a]	41.6±1.76[a,b]	0.58±0.020[a]
BPH group	1.423±0.146[a]	0.058±0.007 [d]	27.4±2.43 [d]	0.40±0.022[c]
Protective group	0.352±0.043[c]	0.103±0.012[c]	38.7±1.33 [b]	0.50±0.035[b]
Curative group	0.783±0.112[b]	0.08±0.002 [e]	33.8±1.56 [c]	0.49±0.051[b]

a, b, c, d & e: There is significant difference (P>0.05) between any two groups, within the same column not having the same superscript letter.

Values are mean±SD. BPH: Benign prostatic hyperplasia; MDA: Malondialdehyde; GSH: Glutathione; SOD: Superoxide dismutase; CAT: Catalase. Statistical analysis was performed by ANOVA, followed by Tukey's post-hoc test. SD: Standard deviation; ANOVA: Analysis of variance.

Table 4. Epithelial height, acinar luminal area, stromal area and PCNA percentage changes

Group	Epithelial height (µm)	Acinar luminal area (μm^2)x 10^3	stromal area (μm^2)x 10^3	PCNA %
Control group	15.55±1.34 [c]	441.89±1.90 [a]	267.40±1.65 [c]	1.25±0.11 [d]
Orchiectomized group	6.23±0.99 [d]	120.00±1.56 [c]	589.74±2.09 [a]	2.28±0.31 [d]
BPH group	23.74±2.96 [a]	330.38±1.63 [b]	380.49±3.90 [b]	32.51±1.70 [a]
Protective group	15.60±1.94 [c]	442.05±1.00 [a]	268.92±3.39 [c]	5.01±1.14 [c]
Curative group	19.51±1.25 [b]	331.11±1.68 [b]	379.28±2.29 [b]	16.17±0.92 [b]

a, b, c & d: There is significant difference (P>0.05) between any two groups, within the same column not having the same superscript letter.

Values are mean±SD. BPH: Benign prostatic hyperplasia; PCNA: Proliferating cell nuclear antigen. Statistical analysis was performed by ANOVA, followed by Tukey's post-hoc test. SD: Standard deviation; ANOVA: Analysis of variance.

Figure 1. Photomicrographs of sections of prostate: **(A&F)** Control group showing normal prostatic tissue, formed of numerous acini (A) lined with a single layer of low columnar epithelium (E) and sparse stroma (s) in between. **(B&G)** Orchiectomized group showing expanded stroma (s), with inflammatory infiltrate (I) and flattened (F) or loss (arrow) of epithelial cells in some acini. **(C&H)** BPH group showing that epithelial hyperplasia markedly narrowing the acinar lumens (L) and produce large involutions (arrows), cell loss in some epithelial areas (L), congested blood vessels (B), other epithelial cells display vacuolations (v), with plentiful stroma in between the acini (s). **(D&I)** Protective group showing that the acini (A) lined with single layer of low columnar epithelium (E) with no involutions and reduced stromal thickness (s). **(E&J)** Curative group showing no involutions, some acini are lined by flat epithelium (F), others have multiple layers of epithelium (thick arrows), and moderate amount of stroma (s). (H&E, Fig. A, B, C, D, E X100 – scale bar = 50 μm; Fig. F, G, H, I, J X400 – scale bar = 25 μm).

Figure 2. Photomicrographs of sections of prostate: **(A)** Control group showing fine collagen fibers (C) dispersed in the stroma between the acini. **(B)** Orchiectomized group showing expanded stroma, with plentiful collagen fiber deposits (C). **(C)** BPH group showing abundance of collagen fibers (C) in the stroma. **(D)** Protective group showing minimal increase in the amount of collagen in the stroma (C). **(E)** Curative group showing moderate collagen deposits (C). (Masson Trichrome X400 – scale bar = 25 μm).

Figure 3. Photomicrographs of sections of prostate: **(A)** Control group showing minimal nuclear immunoexpression (arrows). **(B)** Orchiectomized group showing minimal nuclear immunoexpression in the epithelial cells (arrow). **(C)** BPH group showing pronounced increase in nuclear immunoexpression in the epithelial cells (arrows). **(D)** Protective group showing minimal nuclear immunoexpression in the epithelial cells (arrows). **(E)** Curative group showing moderate nuclear immunoexpression in the epithelial cells (arrows). (PCNA X400 – scale bar = 25 μm).

Figure 4. Electron micrographs of the ventral lobe of prostate gland of control group showing: **A.** normal secretory epithelial cells with oval euchromatic nuclei (N), prominent nucleoli (n), parallel flat endoplasmic reticulum (ER), distinctive cell membranes (arrow) and numerous cytoplasmic electron dense secretory vesicles (S). **B.** Well-developed apical microvilli (m) and the apical region contains many dense secretory vesicles (S). (TEM Fig. A; ×3000 – Scale bar = 2 μm; Fig. B; ×6000 – Scale bar = 1 μm).

Figure 5. Electron micrographs of ventral lobe of prostate gland of orchiectomized group showing: **A.** Secretory cells' nuclei (N) with irregular nuclear envelopes (thick arrows) and hypodense chromatin (arrowhead). The cytoplasm is rarefied (R). Most of secretory vesicles are absent. Cells' boundaries are clearly defined (arrows). **B.** Most of apical microvilli are lost (thick arrows) and few hypodense apical secretory vesicles (S) are noticed. (TEM ×3000 – Scale bar = 2 μm).

Figure 6. Electron micrographs of ventral lobe of prostate gland of BPH group showing: **A.** Several secretory cells can be seen in multiple layers. **B.** The nuclear envelopes (N) of these cells are highly folded and most of the cell boundaries are lost. **C.** the ER is extremely dilated (ER) with absence of most secretory vesicles. **D.** Variable sized intracellular vacuoles can be seen in the secretory cells (V). **E.** Most of the apical microvilli are lost (arrows). (TEM Fig. A; ×1000 – Scale bar = 5 μm; Fig. B,C,E; ×3000 – Scale bar = 2 μm; Fig. D; ×6000 – Scale bar = 1 μm).

Figure 7. Electron micrographs of ventral lobe of prostate gland of protective group showing: **A.** Secretory cells appear arranged in one layer. **B.** Nuclei (N) are normal, but their nuclear envelopes have slight invagination (arrow). The cytoplasm contains secretory vesicles (S) and has slightly dilated ER (ER). The cells have distinct boundaries (arrowheads). **C.** Microvilli (m) are largely restored to normal and secretory vesicles (S) are also increased apically. (TEM Fig. A,B; ×3000 – Scale bar = 2 μm; Fig. C; ×6000 – Scale bar = 1 μm).

Figure 8. Electron micrographs of ventral lobe of prostate gland of curative group showing: **A.** Nuclei (N) of the secretory cells appear irregular, with condensed chromatin (arrowhead) and invaginations on their nuclear envelopes (arrows). The ER has somewhat dilated cisterns (ER). The cells' boundaries were still indistinct. **B.** There are some losses in the apical microvilli and some short microvilli (m). Apical secretory vesicles (S) were also evident in some cells. (TEM ×3000 – Scale bar = 2 μm).

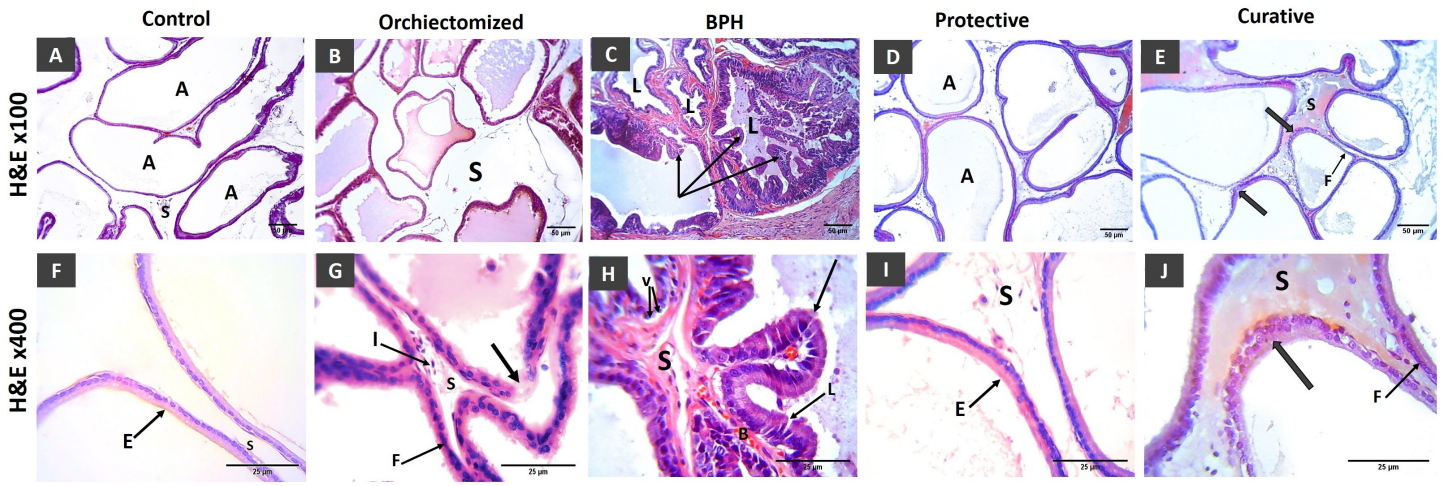
Control
Orchiectomized
BPH
Protective
Curative
H&E x100
H&E x400
A
B
C
D
E
F
G
H
I
J
S
L
E
F
I
V
B

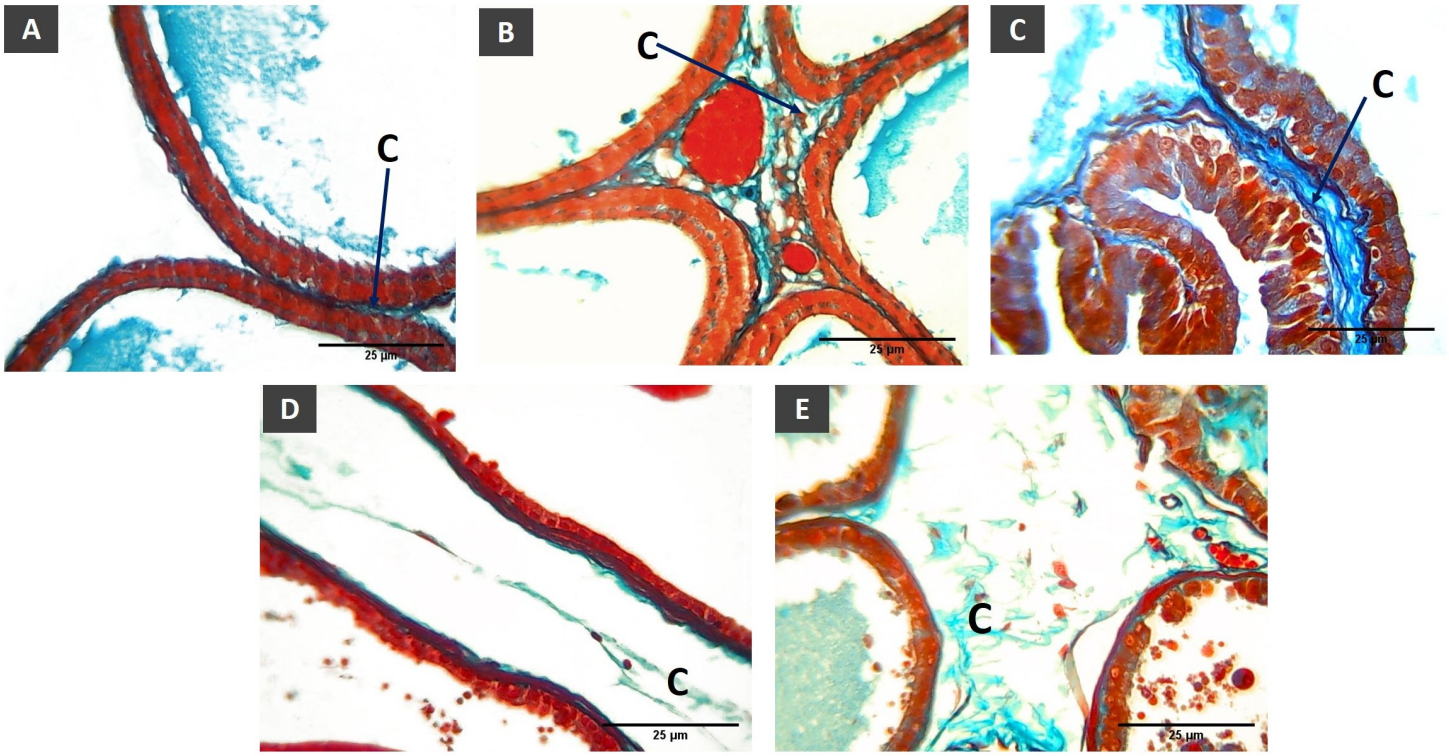
A
C
25 µm
B
C
25 µm
C
C
25 µm
D
C
25 µm
E
C
25 µm

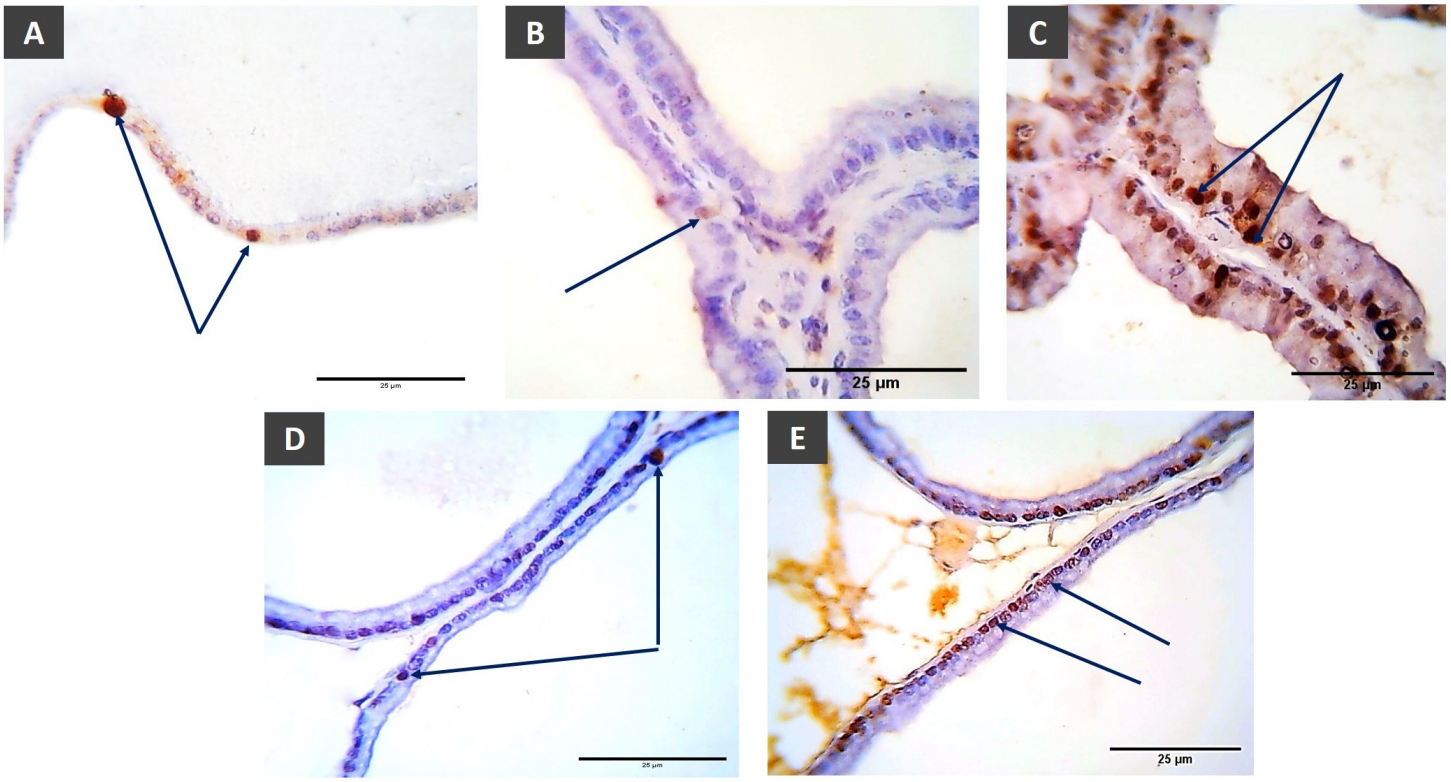
A
B
25 µm
C
25 µm
D
E
25 µm

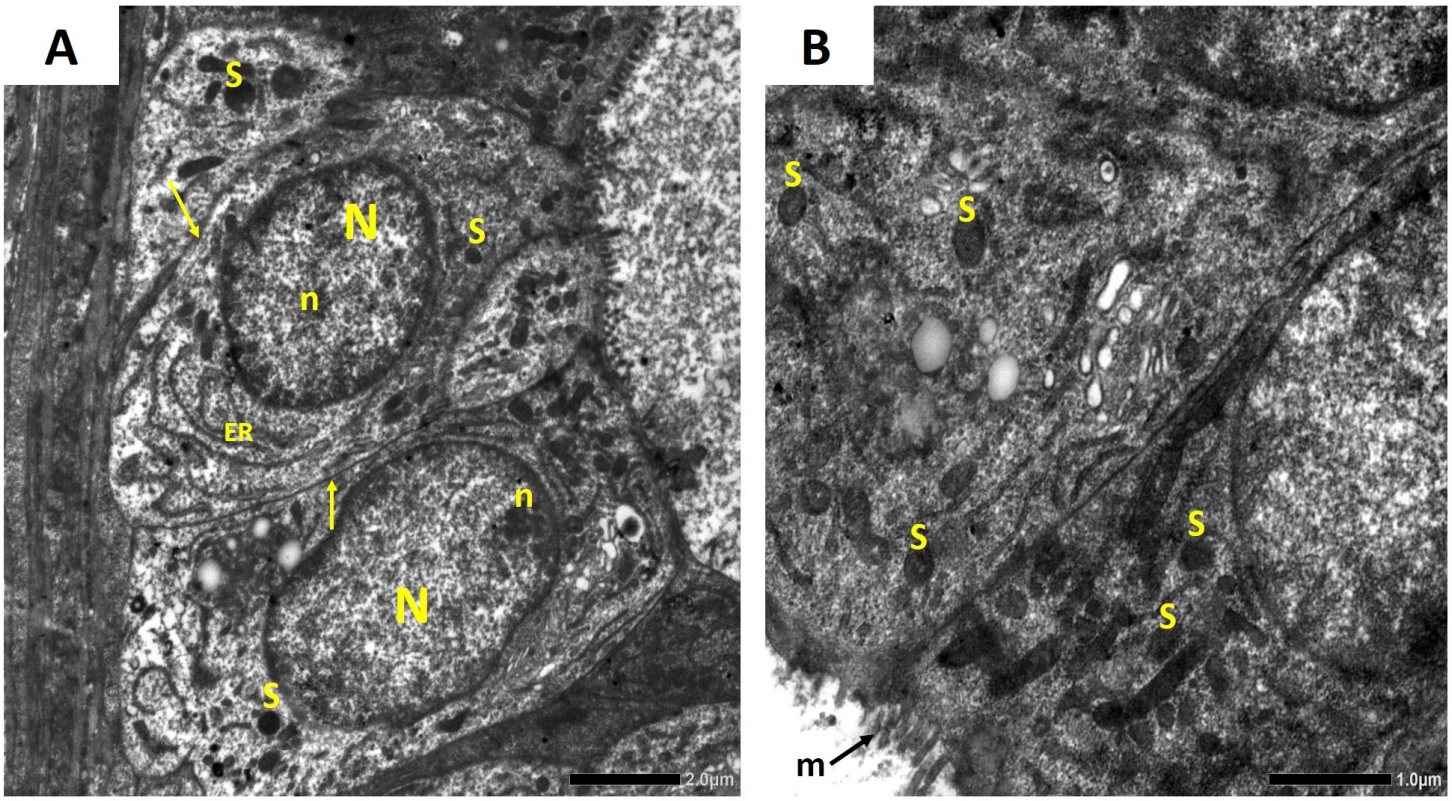
A
S
N
S
n
ER
n
N
S
2.0μm
B
S
S
S
S
S
m
1.0μm

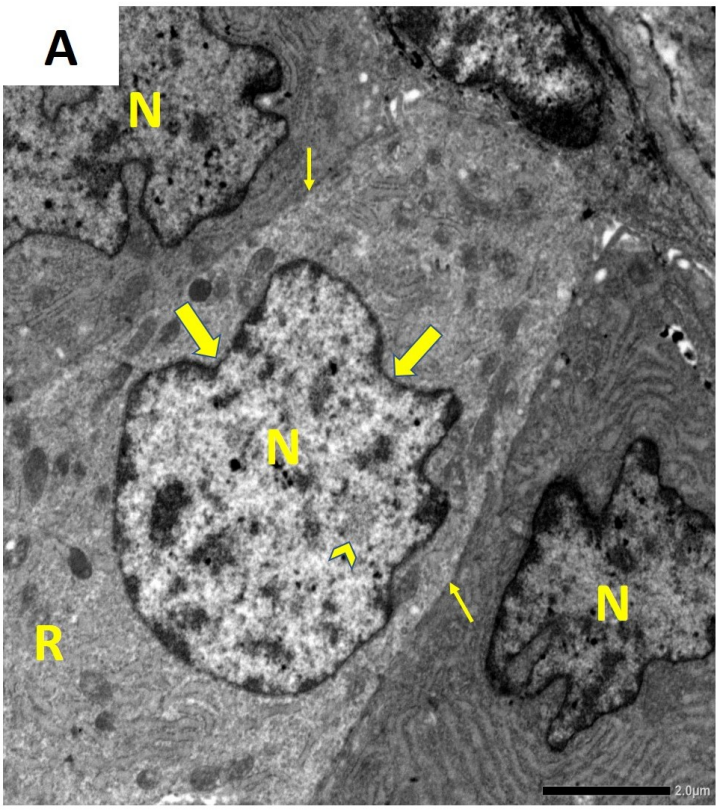
A
N
N
N
R
2.0μm

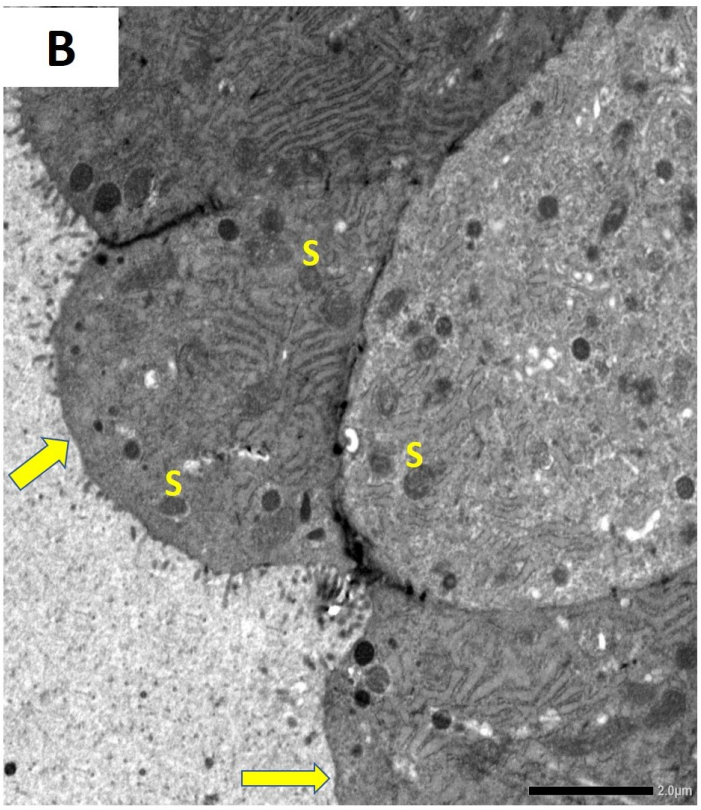
B
S
S
S
2.0μm

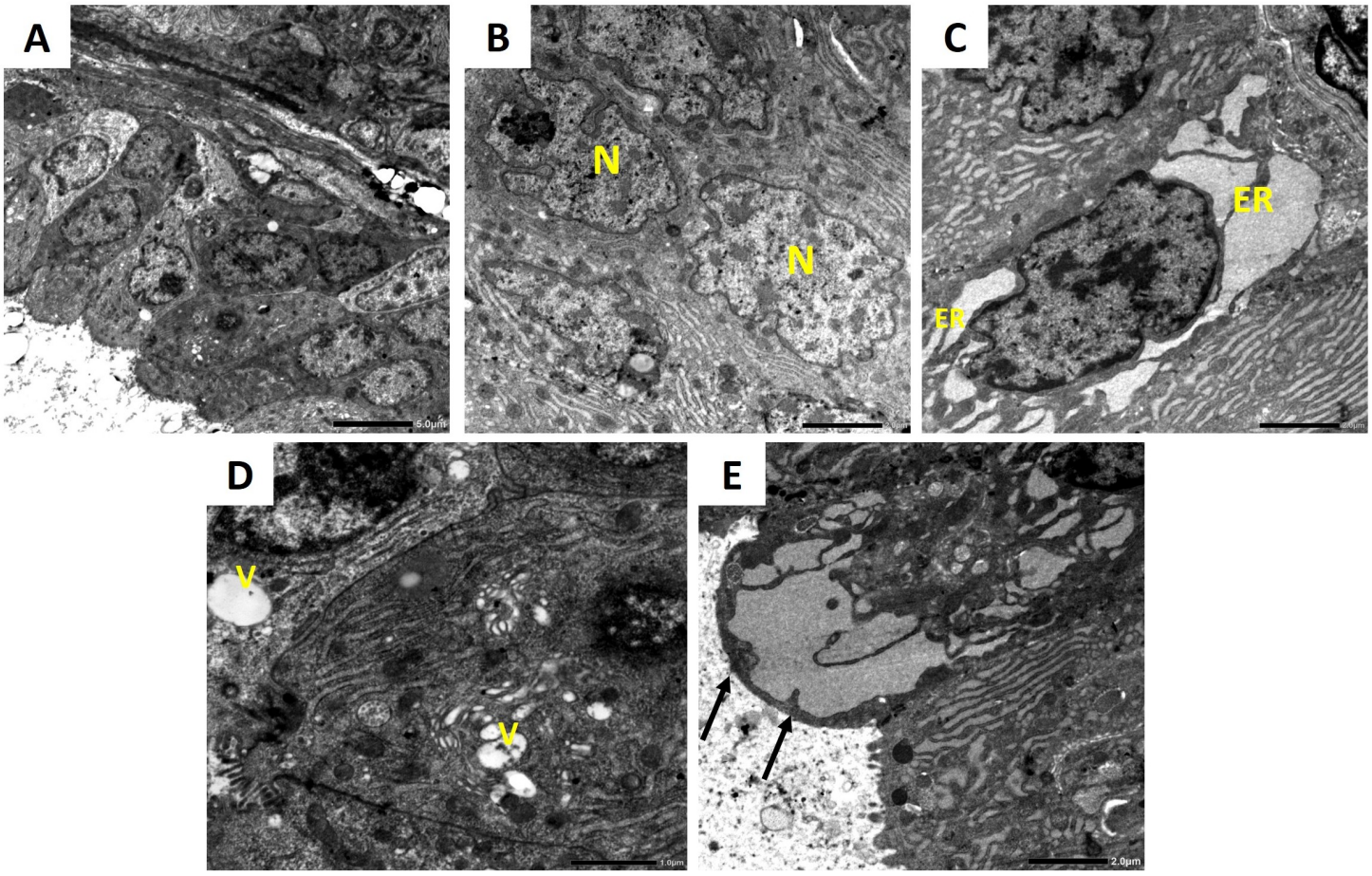
A
B
N
N
C
ER
ER
D
V
V
E
5.0μm
2.0μm

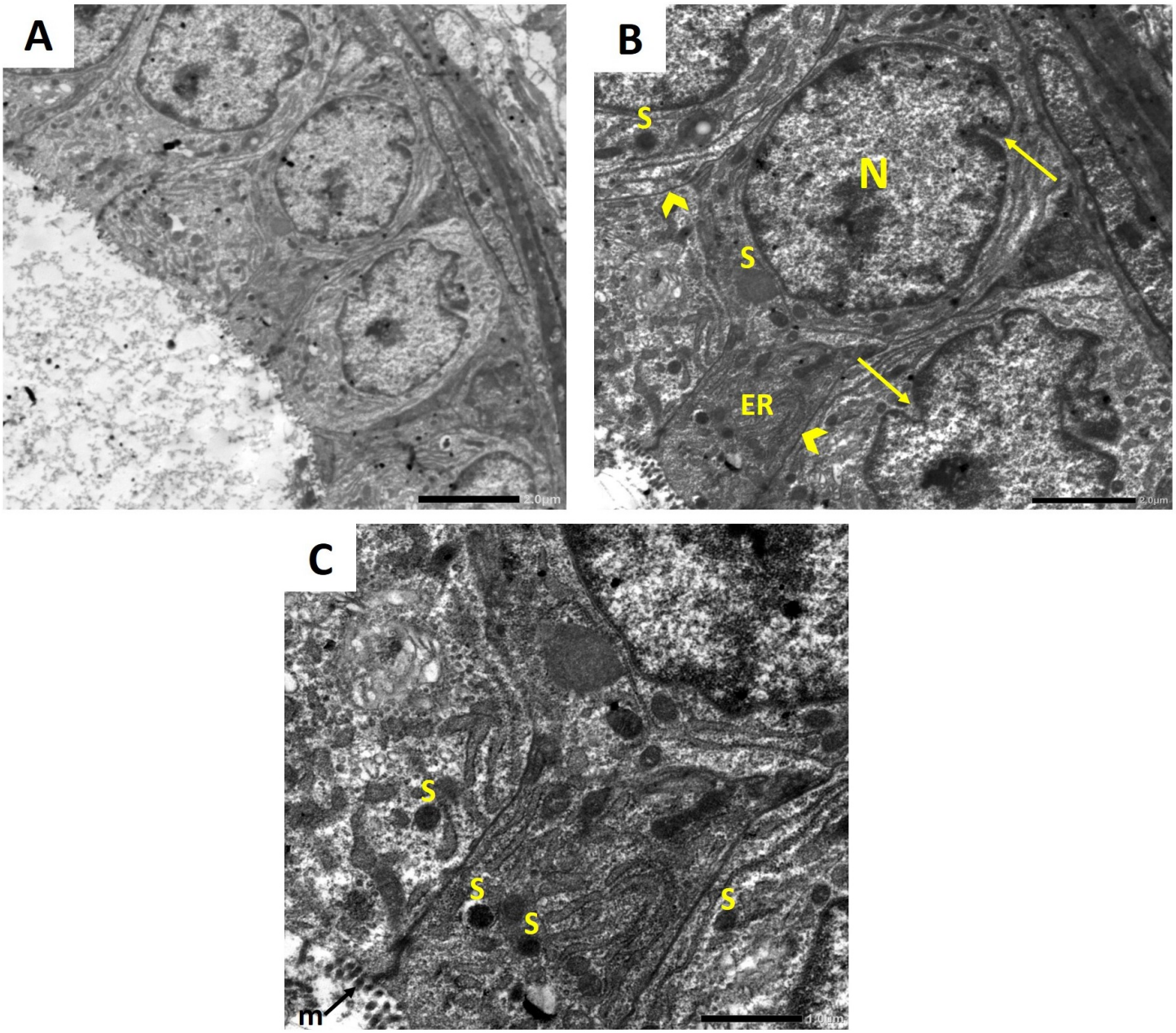
A
B
S
N
S
ER
C
S
S
S
S
m

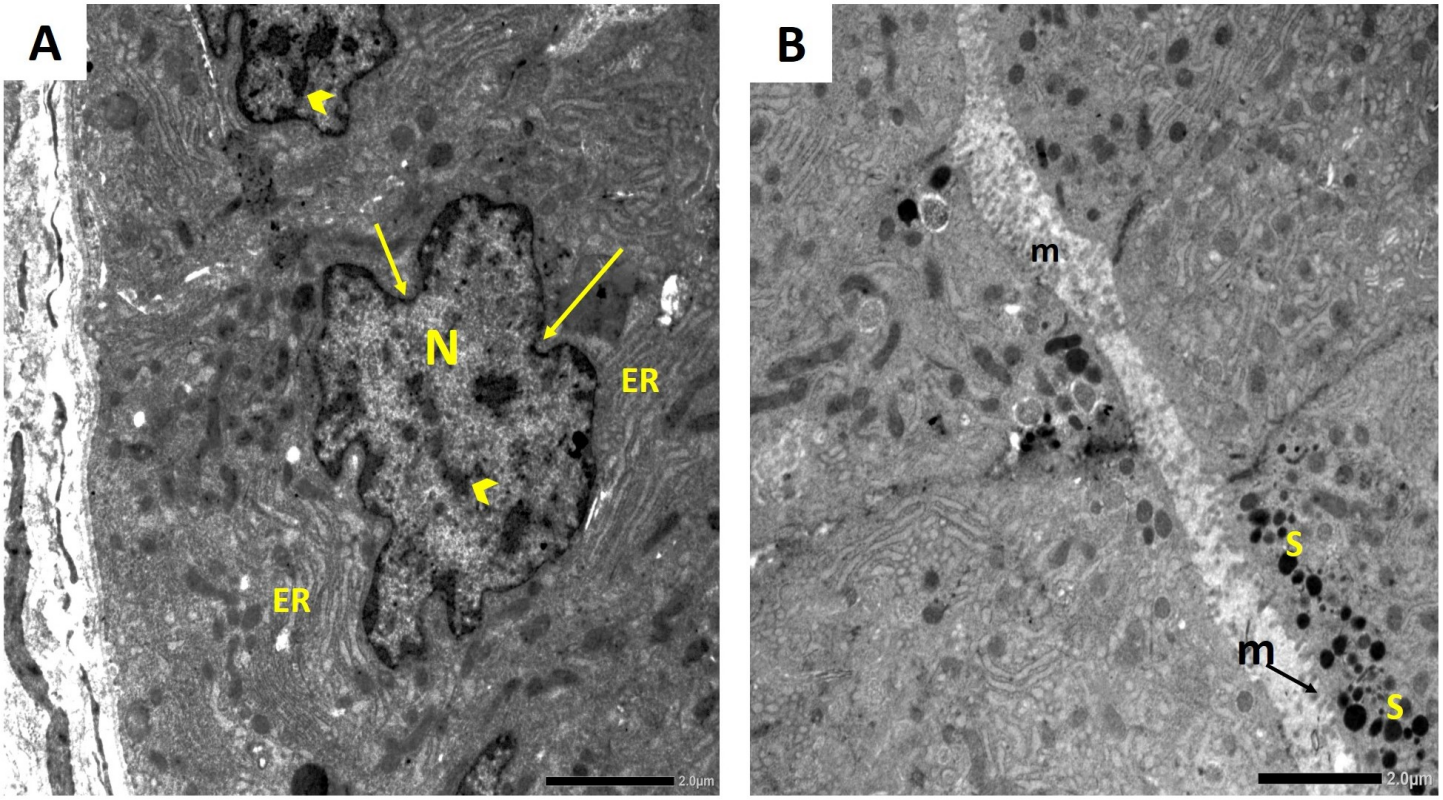
A
N
ER
ER
2.0μm
B
m
S
m
S
2.0μm